processes

MDPI

Article

Eccentricity Analysis of the Co-Excitation Axial Reluctance Resolver during Manufacture and Installation

Hao Wang [1,*], Jundi Wang [2], Zongsheng Zhang [1] and Changchao Li [1]

[1] College of Electrical Engineering and Automation, Shandong University of Science and Technology, Qingdao 266590, China; zhangzongsheng@sdust.edu.cn (Z.Z.); lichangchao12345@163.com (C.L.)
[2] School of Artificial Intelligence, Shenyang University of Technology, Shenyang 110870, China; wangjundi99@163.com
* Correspondence: wanhao1229@163.com; Tel.: +86-13375569946

Abstract: In this paper, a type of co-excitation axial reluctance resolver (CARR) in different winding modes is taken as the simulation model. Detailed explanations have been provided on its stator, rotor, and windings. Simultaneously, an introduction was made to the distribution of two types of signal winding modes. The influence of three kinds of eccentricity on the output characteristics of this CARR during installation and fabrication is also studied. According to two kinds of signal winding modes, the variation law of waveform and amplitude of output potential is analyzed under the conditions of stator radial eccentric distance in different eccentric directions, rotor radial eccentric distance in different eccentric directions and rotor axial offset, and the influence of three factors on total harmonic distortion (THD) is analyzed further. Under the conditions of different eccentricities and offset, a prototype of 15 pair pole CARRs in the mode of sinusoidal windings is tested. The function errors of the signal windings under conditions of radial eccentricity of the stator, radial eccentricity of the rotor and axial offset of the rotor were measured separately. The variation rule of error was compared between measurement and simulation. The correctness of the finite element simulation results under three different eccentricity conditions was verified. The verification results provide theoretical support for further optimization of structural parameters and the installation of the stator and rotor, which can improve measurement accuracy.

Keywords: axial reluctance resolver; co-excitation; eccentricity; finite element simulation

check for updates

Citation: Wang, H.; Wang, J.; Zhang, Z.; Li, C. Eccentricity Analysis of the Co-Excitation Axial Reluctance Resolver during Manufacture and Installation. *Processes* **2024**, *12*, 308. https://doi.org/10.3390/pr12020308

Academic Editor: Wen-Jer Chang

Received: 21 December 2023
Revised: 24 January 2024
Accepted: 27 January 2024
Published: 1 February 2024

Copyright: © 2024 by the authors. Licensee MDPI, Basel, Switzerland. This article is an open access article distributed under the terms and conditions of the Creative Commons Attribution (CC BY) license (https://creativecommons.org/licenses/by/4.0/).

1. Introduction

The structure of resolvers can generally be divided into three types: wound resolvers, radial reluctance resolvers, and axial reluctance resolvers. As a position sensor in a servo motor control system, the resolver can be used in many fields such as robots, electric vehicles, aviation and aerospace [1–5]. The wound resolver realizes a sinusoidal electromagnetic field through the excitation windings distribution set on the rotor [6]. The windings of the other two kinds of resolvers are arranged on the stator, and the sinusoidal variation law of the electromagnetic field is realized by changing the coupling area or the air gap length between the stator and the rotor [7,8]. The electrical error of one pole pair wound resolver is relatively low and can reach $\pm 10'$. The volume of one pole pair reluctance resolver is smaller than that of one pole pair wound resolver, and the electrical error is relatively large and can reach $\pm 60'$.

The design purpose of resolvers is to achieve accurate measurement of the position or angle. Therefore, in the design process, it is necessary to consider the spatial position coordination with the tested motor, and different structural designs should be completed for different tested objects [9–11]. On the basis of completing the preliminary design of the resolvers, further structural optimization is needed, and the optimization method is limited by design requirements and the installation environment. Ref. [12] achieved

accuracy compensation by changing the tooth shape through the tooth-pairing method. In [13], a Fourier series is used to optimize the shape of the rotor, and the correctness of the optimization is verified by finite element analysis. On the basis of the structural design and optimization, the resolver will also conduct research on certain characteristics, which typically include the winding configuration and inductance characteristic analysis. In [14], the anti-interference of the sinusoidal distributed winding configuration is verified using the winding function method, and the results of the proposed method under constant and sinusoidal distributed winding configurations are compared with the finite element method in terms of accuracy and computation costs. The winding function method can not only configure the winding distribution law, but also be applied to calculate the inductance of the internal winding with resolvers and analyze the harmonic distribution of the signal output in principle [15]. In [16], a novel self-correction composite method based on a discrete extended state observer and a harmonic observer method is put forward to calibrate the angular position of the resolver. The verification results indicate that this method can improve measurement accuracy. In addition, the eccentricity issue during installation and processing is also one of the factors affecting the measurement accuracy of resolvers [17]. In [18], the measurement error is reduced and the error caused by the rotor eccentricity is suppressed by building an analytical current model. In [19], the Siamese network was used to detect the static eccentricity voltage of each tooth of the resolver, and the eccentricity position was extracted by converting it into a rotor angle.

At present, most of the research on resolvers is mainly focused on the structure and winding distribution of the stator and rotor [20–22]. However, there are still some other problems affecting the accuracy that need to be solved, and which can be summarized as the following three aspects:

(1) Errors in the processing: The main reason is that the radial and axial reluctance resolvers have complex corrugated rotor structures, resulting in high processing difficulty, high technical requirements, and easy occurrence of rotor deformation, eccentricity, and other problems.

(2) Limitations to the coordination of poles and slots: The pole pairs of the resolver and the tested motor need to be designed in conjunction, which cannot fully follow the design concept of the resolver. Moreover, the given space size further limits the stator design and distribution of the winding turns [23–25].

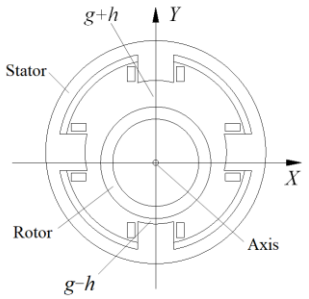
(3) Strict installation requirements: The stator and rotor need to be installed strictly in accordance with the coaxial fixation. And the radial eccentricity and axial offset may affect the accuracy [26].

Based on the above problems, this paper takes the CARR as the research object, and analyzes the amplitude of the output electromotive force (EMF) and the total harmonic distortion (THD) according to the stator radial eccentricity, rotor radial eccentricity and rotor offset under two different winding modes. This provides a certain reference for the design and optimization of the reluctance resolver. The three eccentricities are shown in Figure 1. By summarizing the completed research, the main contributions of this research are as follows:

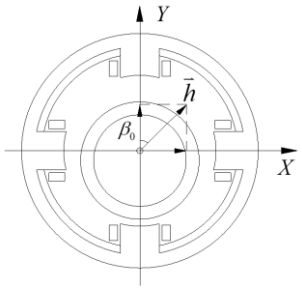
(1) The structure of the CARR is introduced. The distribution law and setting mode of four phase signal windings under two winding types are explained in detail.

(2) The stator radial eccentricity, rotor radial eccentricity and rotor offset under different eccentricity directions are simulated and analyzed. The variation trends of the signal output EMF amplitude and harmonic distortion rate were compared and analyzed under two winding types.

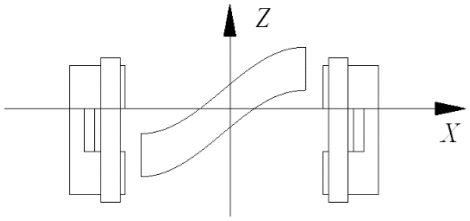
(3) Precision measurements were conducted on a prototype of 15 pole pairs of CARRs in the sinusoidal winding mode. The function errors of the precise machine signal output and coarse machine signal output were compared and analyzed under three working conditions: stator radial eccentricity, rotor radial eccentricity and rotor axial offset.



(**a**) Radial eccentricity of stator



(**b**) Radial eccentricity of rotor



(**c**) Axial offset of rotor

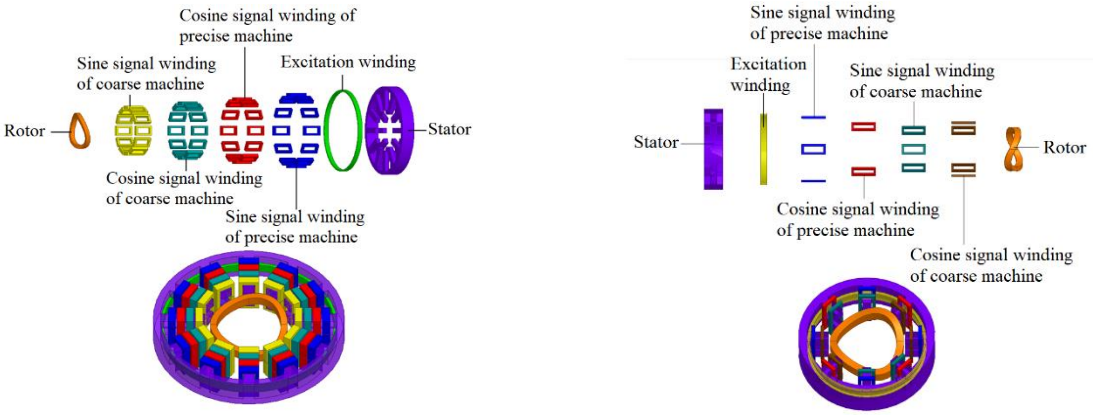
Figure 1. Three types of eccentricity diagrams.

The research work of this paper is based on the published papers "Electromagnetism Principle of the Coarse-Exact Coupling Variable-Reluctance Resolver" and "The Analysis of Multipole Axial Flux Reluctance Resolver with Sinusoidal Rotor", which have provided a detailed introduction to the model structure and basic principles of the CARR. Therefore, the specific simulation methods and waveform generation process of the output EMF will not be discussed here. In this paper, the eccentricity and offset of the stator and rotor of the CARR are simulated and analyzed, and the error variation law of the signal output is established, and this provides a reference for the design and optimization of this kind of resolver.

2. Effect of Eccentricity and Offset of Stator and Rotor on Output Electromotive Force

The CARR is a multi-pole brushless reluctance resolver, which is suitable for speed and position sensors of servo systems.

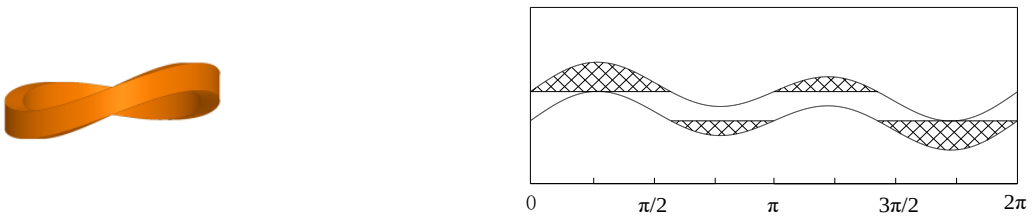
The CARR is composed of a stator and a rotor. And the equal air gap is set between the stator and the rotor. There are 4*NP* identical slots on the inner side of the stator. A through slot is set along the circumference of the stator. The stator has 4*NP* upper teeth and 4*NP* lower teeth. *N* is a natural number. The excitation winding is the ring winding which is set in the stator slot. And the excitation winding is concentric with the stator. Figure 2a is the schematic diagram of the CARR in the sinusoidal winding mode. The sine signal windings of the coarse machine are divided into two groups. The first group is wound anticlockwise on adjacent *NP* stator teeth. The second group is wound clockwise on other adjacent *NP* stator teeth. The setting mode of the sine signal windings and cosine signal windings of the coarse machine is the same. The difference between the two signal windings is that the phase difference is a 90° electrical angle. The sine signal windings of the precise machine are divided into 2*P* groups. The first group is wound anticlockwise on adjacent *N* stator teeth. The second group is wound clockwise on other adjacent *N* stator teeth. The other groups are set in the same way until the 2*P* groups sine signal windings of the precise machine are set completely. The setting mode of the sine signal windings and cosine signal windings of the precise machine is the same. The difference between the two signal windings is that the phase difference is a 90° electrical angle.



(**a**) The sinusoidal winding mode (**b**) The winding mode of equal turns

Figure 2. Three-dimensional model of two pole pairs of CARRs.

In terms of the structure, the difference between the CARR in two different winding modes lies in the distribution of the signal windings. Figure 2b is the schematic diagram of the CARR in the winding mode of equal turns. The magnetic conductive part of the rotor core which is designed with an optimization function of magnetic field is a multipole strip magnetic conductive structure. The rotor structure is shown in Figure 3.



(**a**) Structural diagram of rotor (**b**) Plane expansion diagram of rotor

Figure 3. Rotor schematic diagram of two pole pairs of CARRs.

This paper mainly studies the radial eccentricity of the stator, the radial eccentricity of the rotor and the axial offset of the rotor in the installation process of this new type of CARR. The influence of different eccentricities and offset on the measurement accuracy of signal output is analyzed.

2.1. Effect of Stator Radial Eccentricity

Stator radial eccentricity is the situation where the rotor of the resolver is concentric with the rotating shaft and the stator deviates from the rotating shaft because of factors such as the silicon steel sheet lamination, fixation with the mechanical structure of the outer shell, and installation of the stator in coordination with the rotor, as shown in Figure 1a. The CARR has a special structure, which is more vulnerable to the influence of eccentricity. So, it is necessary to analyze different eccentric situations. When the stator and rotor are relatively stationary, the eccentricity distance of the stator along a certain stator tooth axis is h. In the case of non-eccentricity, the length of the air gap between the stator and rotor is g. When the stator is eccentric, the length of the air gap between the stator and rotor does not change with the rotation angle. However, the air gap length of the stator eccentricity corresponding to each stator tooth is no longer equal.

The maximum length of the air gap caused by the radial eccentricity of the stator is $g + h$, which occurs at the position of the first stator tooth axis, and the minimum value is $g - h$, which occurs at the stator tooth axis at a mechanical angle of 180 degrees with the

first tooth. The length of the air gap distributed by other teeth according to their positions can be expressed as

$$g_i = \left(h^2 + 2hg\cos\left((i-1)\cdot\frac{2\pi}{Z_s}\right) + g^2\right)^{\frac{1}{2}} \quad (1)$$

The change in the air gap will change the magnetic conductance of the air gap corresponding to each stator tooth and this affects the output electromotive force of the signal windings. In the case of the stator radial eccentricity, the magnetic conductance of the air gap corresponding to each stator tooth can be expressed as:

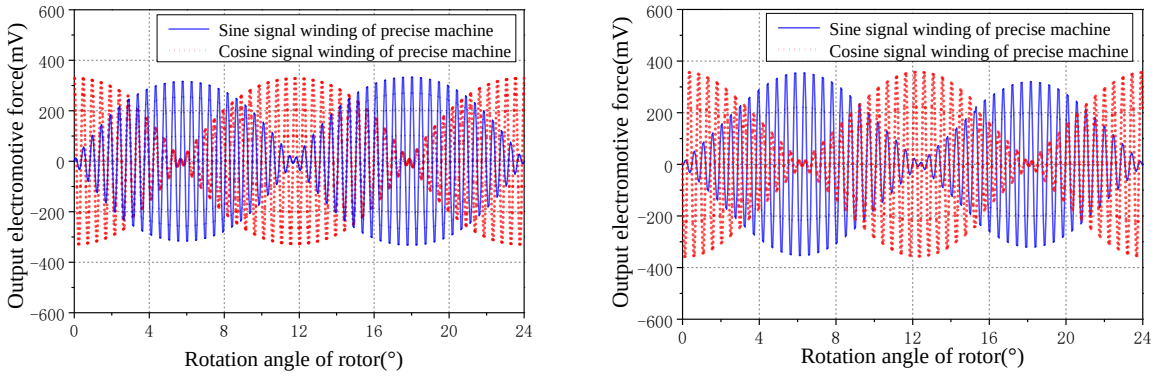
$$\begin{aligned}\Lambda_i &= \Lambda_0 + \Lambda_{i1} + \Lambda_{iP} \\ &= \Lambda_0 + \mu_0 \cdot S_{i1}/g_i + \mu_0 \cdot S_{iP}/g_i\end{aligned} \quad (2)$$

In Formulas (1) and (2), i is the serial number of the stator teeth. Λ_0 is the constant component of the air gap magnetic conductance. Λ_{i1} is the fundamental component of the air gap magnetic conductance. Λ_{iP} is the harmonic component of the air gap magnetic conductance. μ_0 is the air permeability. g is the air gap length of the stator and rotor. h is the eccentricity distance of the stator and rotor. S_{i1} is the equivalent fundamental component of the coupling area. S_{iP} is the equivalent harmonic component of the coupling area. Z_s is the number of stator teeth.

It can be seen from Formula (2) that the change in air gap length will directly affect the air gap magnetic conductance corresponding to each stator tooth. Therefore, the change law of the output electromotive force of four phase signal windings is also different from that of the stator without radial eccentricity.

The finite element method of the electromagnetic field is used to simulate and analyze the variation in the output electromotive force of signal windings when the stator is eccentric in different directions. In the finite element software, models of 15 pole pairs of CARRs in the winding mode of equal turns and sinusoidal winding mode are established, respectively.

With an eccentricity of 0.6mm, the output EMF of the precise machine signal windings of 15 pole pairs CARRs in different winding modes is shown in Figure 4.



(**a**) The type of equal turns winding (**b**) The type of sine winding

Figure 4. Variation law of signal windings output EMF of precise machine when radial eccentricity of stator exists.

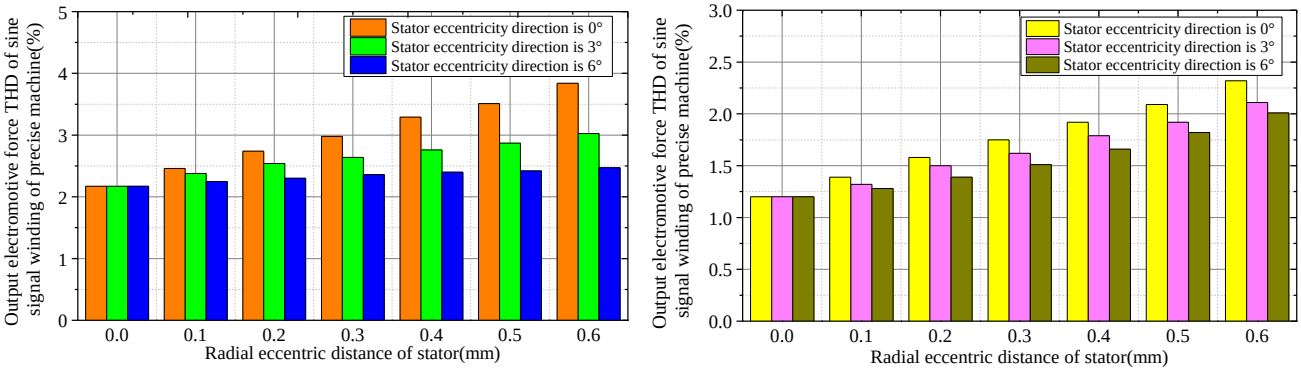
There is no obvious amplitude error between the output electromotive force of the sine signal windings and cosine signal windings of the precise machine in Figure 4, which shows that the radial eccentricity of the stator has little additional impact on the amplitude error between the output electromotive force of two phase signal windings of the precise machine. The simulation results show that the radial eccentricity of the stator will change the zero position of the output electromotive force of precise machine signal windings

and cause an additional zero position error. This is because the radial eccentricity of the stator makes the air gap between the stator and rotor no longer equal and changes the distribution of the air gap magnetic conductance corresponding to each stator tooth. The change in air gap magnetic conductance will mean that the maximum value of the output electromotive force of sine and cosine signal windings in the first half period is not equal with the maximum value of the output electromotive force of sine and cosine signal windings in the last half period. When stator radial eccentricity occurs, the change rule of the output electromotive force of signal windings in the sinusoidal winding mode is the same as that in the winding mode of equal turns.

The amplitude and total harmonic distortion of the output electromotive force of the precision machine sine signal windings in different winding modes are analyzed respectively when the radial eccentricity direction of the stator is 0°, 3°, and 6°. The analysis results are shown in Table 1 and Figure 5. The amplitude of the output electromotive force of precise machine sine signal windings will increase with the increase in the stator eccentricity distance. And the values of the functional error vary with different eccentric directions. At the same time, with the increase in the eccentric distance, the function error of the output electromotive force of the precision machine signal windings shows an upward trend. Comparing the analysis results shown in Table 1 and Figure 5, it is found that analysis results in both winding modes are affected by the radial eccentricity of the stator. However, different radial eccentric directions of the stator have a great influence on the function error of the output electromotive force of precise machine signal windings in the winding type of equal turns. And it has little influence on the function error of the output electromotive force of precise machine signal windings in the sinusoidal winding mode.

Table 1. Amplitude variation law of sine signal winding output EMF of precise machine when radial eccentricity direction of stator is 0°.

Radial Eccentricity Distance (mm)	Amplitude of Output EMF (mV)	
	Equal Turns Windings	Sine Windings
0	299.5	321.9
0.1	302.2	323.0
0.2	306.0	325.9
0.3	310.4	332.0
0.4	316.3	337.0
0.5	322.2	343.7
0.6	328.9	353.5



(**a**) The type of equal turns winding (**b**) The type of sine winding

Figure 5. THD variation law of sine signal winding output EMF of precise machine when radial eccentricity direction of stator changes.

In the case of no eccentricity, the output characteristics corresponding to both the equal turns winding type and sine winding type should maintain a symmetrical waveform, and the envelope of the output EMF should be close to the standard sinusoidal waveform, so as to achieve high measurement accuracy [7,14,15]. The condition of the stator radial eccentricity has a significant impact on the output characteristics of the equal turns winding type and sine winding type. The envelope of the output EMF of the equal turns winding type presents a flat waveform and has a large THD. The envelope of the output potential in the sine winding type is closer to the sinusoidal waveform and has a smaller THD. The peak values of the output EMF are no longer equal in one electrical cycle, and there is an obvious zero offset, which will directly increase the measurement error of the CARR.

2.2. Effect of Rotor Radial Eccentricity

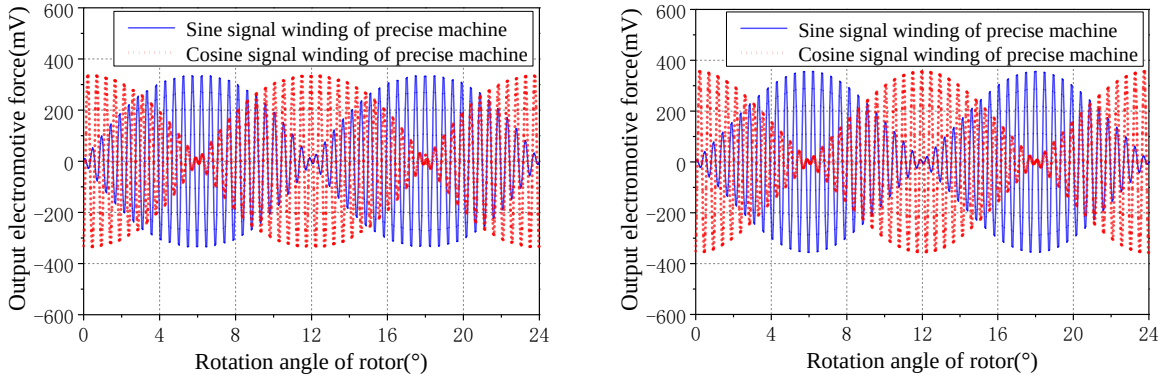
Rotor radial eccentricity is the situation where the stator of the resolver is concentric with the rotating shaft and the center of the rotor deviates from the rotating shaft as a result of factors such as the rotor processing and installation, as is shown in Figure 1b. Different from the stator radial eccentricity, the air gap between the stator and the rotor will change with the rotation of the rotor when the rotor radial eccentricity occurs and the included angle between the rotor radial eccentricity direction and the Z-axis is β_0. The eccentricity is $\overrightarrow{h}$, and its size is h. With the change in the rotation angle, $\overrightarrow{h}$ will also rotate synchronously with the rotor, and the included angle with the Z-axis is $\theta + \beta_0$. Therefore, the air gap length corresponding to each stator tooth changes with the change of angle θ. However, the air gap length corresponding to each position of the rotor is independent of the rotation angle.

Based on the Z-axis, the air gap between the stator and rotor can be expressed as:

$$g' = g - \frac{h}{2} - \frac{h}{2} \cdot [\cos P(\theta - \beta_0) + \cos(\theta - \beta_0)] \tag{3}$$

In the formula, g' is the length of the air gap between the stator and rotor when the rotor is radially eccentric.

In order to obtain the influence of the rotor radial eccentricity on the CARR more clearly, 15 pole pairs of CARRs are taken as the analysis objects. The center line of the maximum wave crest of the rotor is selected as the 0 °direction of the rotor radial eccentricity, and the given eccentricity is 0.6mm. The waveform of the output electromotive force of precise machine signal windings is obtained, as is shown in Figure 6. The finite element analysis of the rotor radial eccentricity along 0°, 3°, and 6° was carried out, and the analysis results are shown in Table 2 and Figure 7.



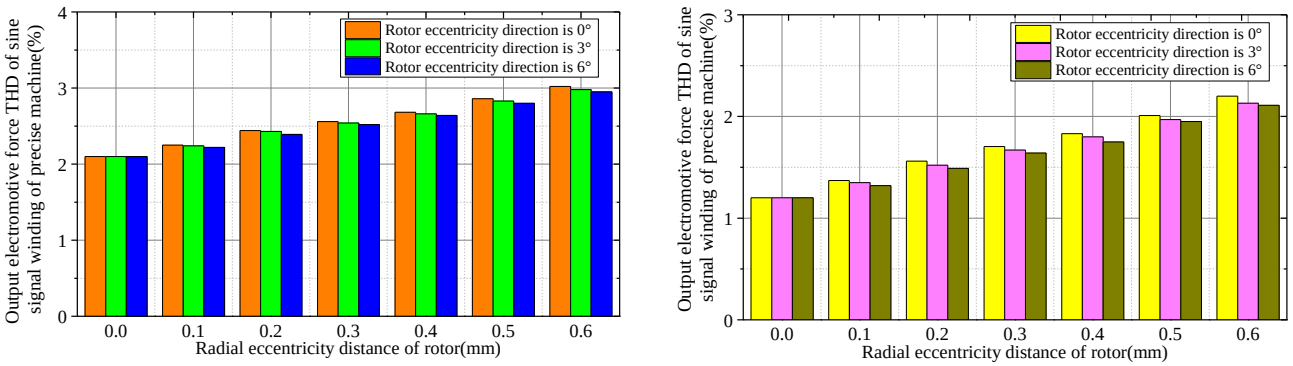
(**a**) The type of equal turns winding (**b**) The type of sine winding

Figure 6. Variation law of signal windings output EMF of precise machine when radial eccentricity direction of rotor is 0°.

The analysis results show that the amplitude of the output electromotive force of the precise machine signal windings changes slightly when the direction of the rotor radial eccentricity is different. In different winding modes, the zero point of the output electromotive force of precise machine signal windings does not change, so no additional zero position error is generated. The amplitude of the output electromotive force of the two-phase precise machine signal windings is the same, so no additional amplitude error is generated. It can be seen from Table 2 and Figure 7 that the amplitude and total harmonic distortion of the output electromotive force of precise machine sine signal windings in two winding modes show an upward trend with the increase in the rotor radial eccentricity distance. For different rotor radial eccentricity directions, the total harmonic distortion variation trend of the output electromotive force of precise machine sine signal windings is basically the same.

Table 2. Amplitude variation law of sine signal winding output EMF of precise machine when radial eccentricity direction of rotor is 0°.

Radial Eccentricity Distance (mm)	Amplitude of Output EMF (mV)	
	Equal Turns Windings	Sine Windings
0	299.5	321.9
0.1	301.2	324.0
0.2	304.3	326.9
0.3	308.6	332.2
0.4	314.9	338.1
0.5	322.6	346.1
0.6	332.8	355.5



(**a**) The type of equal turns winding (**b**) The type of sine winding

Figure 7. THD variation law of sine signal winding output EMF of precise machine when radial eccentricity direction of rotor changes.

Based on the above analysis of the rotor radial eccentricity, it can be seen that the rotor radial eccentricity will cause additional function error in the output electromotive force of precise machine signal windings, but it will not cause an additional zero position error and amplitude error.

2.3. Effect of Rotor Axial Offset

Rotor axial offset is the situation where the stator center (or rotor center) is axially offset relative to the center point of the resolver as a result of the installation of the stator in coordination with the rotor, as shown in Figure 1c. When the axial displacement of the rotor occurs in the CARR, the air gap length between the stator and rotor remains the same, but the coupling area between the stator teeth and magnetic conductive part of the rotor changes. It can be seen that the axial offset of the rotor will change the coupling area

between a single stator tooth and the rotor. Therefore, it is necessary to further analyze the influence of the rotor axial offset on the output electromotive force.

According to the corresponding relationship between the stator teeth and rotor in Figure 8 below, the coupling area between one tooth of the stator and the rotor in the case of the axial eccentricity of the rotor can be approximated as follows:

$$S = H_1 \cdot \sin(\theta) + H_P \cdot \sin(P\theta) + K,\ 0 \le \theta \le 2\pi \tag{4}$$

$$H_1 = 2R \cdot l_1 \cdot A_1 \cdot \sin\left(\frac{b}{2}\right) \tag{5}$$

$$H_P = \frac{2}{P} R \cdot l_1 \cdot A_P \cdot \sin\left(\frac{Pb}{2}\right) \tag{6}$$

$$K = 4R \cdot l_1 \cdot [\beta - \sin(\beta)] + lR(b - 4\beta) \tag{7}$$

In the formula, A_1 is the ratio of the amplitude of the rotor coarse machine function to the axial thickness of the rotor. A_P is the ratio of the amplitude of the precision machining function of the P pole pairs rotor to the axial thickness of the rotor. l_1 is the height of the stator teeth. R is the inner diameter of the stator teeth. b is the tooth width of the stator teeth. l is the axial eccentricity of the rotor. θ is the rotation angle of the rotor.

It can be seen that the coupling area of axial eccentricity has a constant component K on the basis of one pole pair sinusoidal component and a P pole pairs sinusoidal component, and the magnitude of K is related to the eccentricity l. The constant component in the coupling area will be reflected in the air gap permeability, increasing the constant component of the air gap permeability. The constant component in the air gap magnetic conductivity cannot form the output EMF. Meanwhile, there will be no constant component generated in the output EMF.

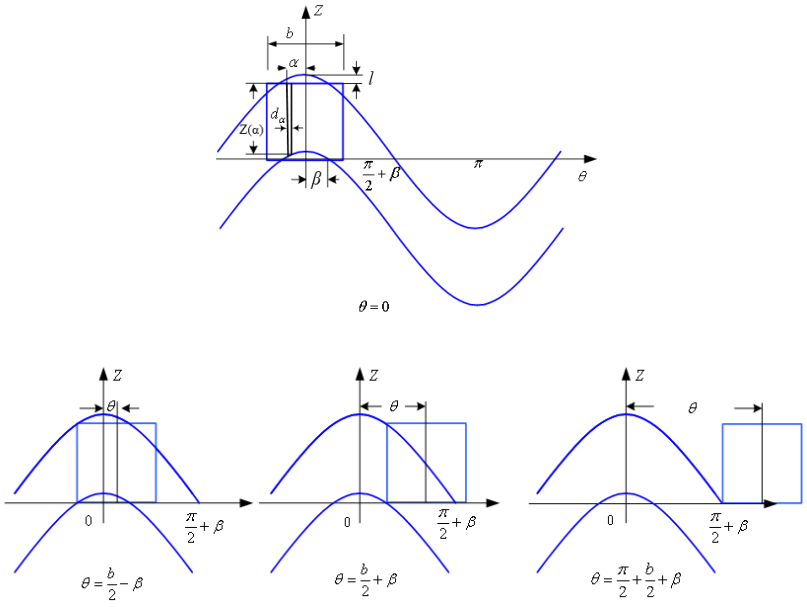
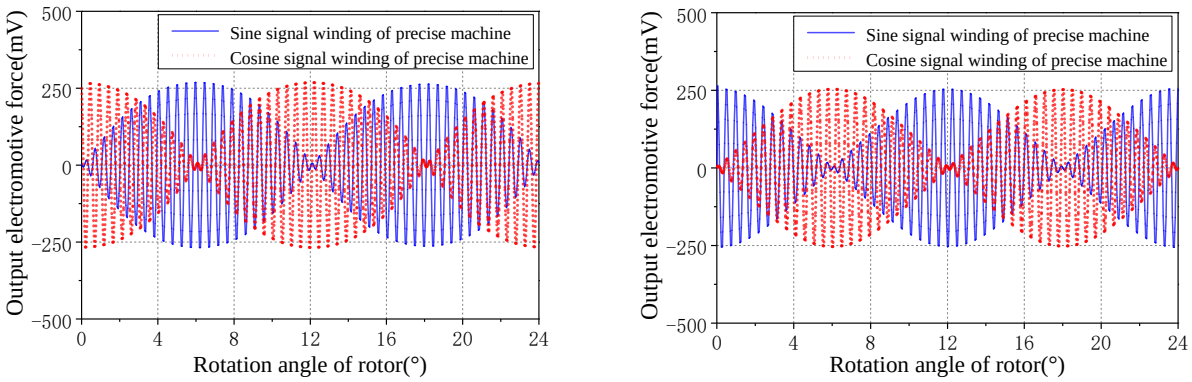


Figure 8. Position relation diagram of stator and rotor when axial offset of rotor exists.

In the case of the rotor axial offset, the finite element analysis is carried out for the 15 pole pairs of the CARR with the winding mode of equal turns and the sinusoidal winding mode, respectively. When the tooth height of the stator is 5 mm, the axial eccentricity of the rotor is 2.4mm, and the waveform of the output electromotive force of the precise machine signal windings is shown in Figure 9. Table 3 and Figure 10 show the amplitude and total harmonic distortion of the output electromotive force of the precise machine signal windings.



(**a**) The type of equal turns winding (**b**) The type of sine winding

Figure 9. Variation law of signal windings output EMF of precise machine when axial offset of rotor exists.

Table 3. Amplitude variation law of sine signal winding output EMF of precise machine when axial offset of rotor changes.

Axial Offset Distance (mm)	Amplitude of Output EMF (mV)	
	Equal Turns Windings	Sine Windings
0	299.5	321.5
0.4	298.0	320.2
0.8	295.4	316.4
1.2	291.0	312.8
1.6	279.1	299.6
2.0	266.5	286.7
2.4	252.9	267.8

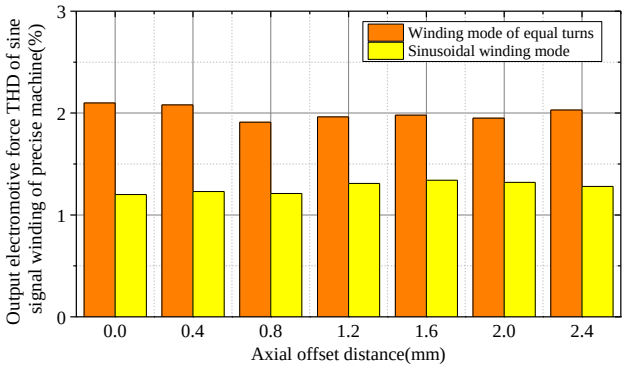


Figure 10. THD variation law of sine signal winding output EMF of precise machine when axial offset of rotor changes.

From the analysis results in Figure 10, it can be seen that there is no obvious amplitude error in the output electromotive force of the signal windings of the precise machine in the two winding modes. Considering the calculation error of the software, when the axial offset of the rotor is less than 50% of the stator tooth height, the axial offset of the rotor will not cause an additional amplitude error of the output EMF of the precise machine signal windings. The zero output electromotive force of the precise machine sine signal winding is π and 2π, and the zero output electromotive force of the precise machine cosine signal winding is $\pi/2$ and $3\pi/2$. It can be seen that there is no zero error in the output electromotive force of signal windings of the precise machine in the two winding modes.

The analysis results in Table 3 show that the amplitude of the output electromotive force of the precise machine signal windings will decrease with the increase in the axial

offset of the rotor. When the amplitude of the signal winding function of the precise machine in two winding modes is equal, the amplitude of the output electromotive force of precise machine signal windings in the sinusoidal winding mode is always larger than that in the winding mode of equal turns.

In Figure 10, when the axial offset of the rotor is within 50% of the stator tooth height, the total harmonic distortion of the output electromotive force of precise machine signal windings is basically unchanged. Therefore, it can be considered that when the offset is less than 50% of the stator tooth height, the rotor axial deviation will not cause an additional function error.

3. Measurement Accuracy Experiment of CARR

As the CARR is a kind of position sensor, it has strict requirements of measurement accuracy. After theoretical derivation and finite element analysis, it is necessary to measure the characteristics of the prototype in actual work and compare them with the finite element simulation results.

A total of 15 pole pairs of CARRs are selected for the experimental prototype. The sinusoidal winding mode is adopted. The prototype structure is shown in Figure 11. Figure 12 shows the experimental platform for the precision measurement, which is composed of an oscilloscope, a function signal generator, a grating dividing head and a mechanical rotating platform. Among them, the measurement accuracy of the dial gauge is generally 0.001 mm, which meets the experimental measurement requirements. The measurement accuracy of the grating dividing head can reach 1″, which meets the requirements of the prototype experiment conducted in this paper. The function error and zero position error of these 15 pole pair CARRs under the conditions of stator radial eccentricity, rotor radial eccentricity and rotor axial deviation will be measured. And the correctness of the simulation results will be verified.



(**a**) Stator structure (**b**) Rotor structure

Figure 11. Prototype structure diagram of 15 pole pairs coarse and precise coupling axial reluctance resolver.

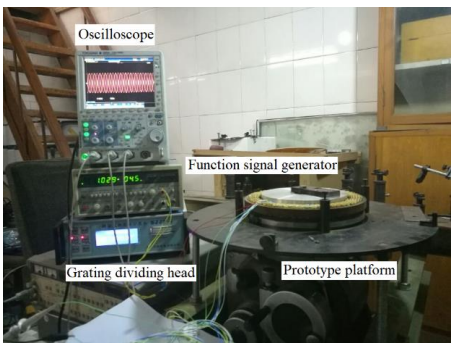
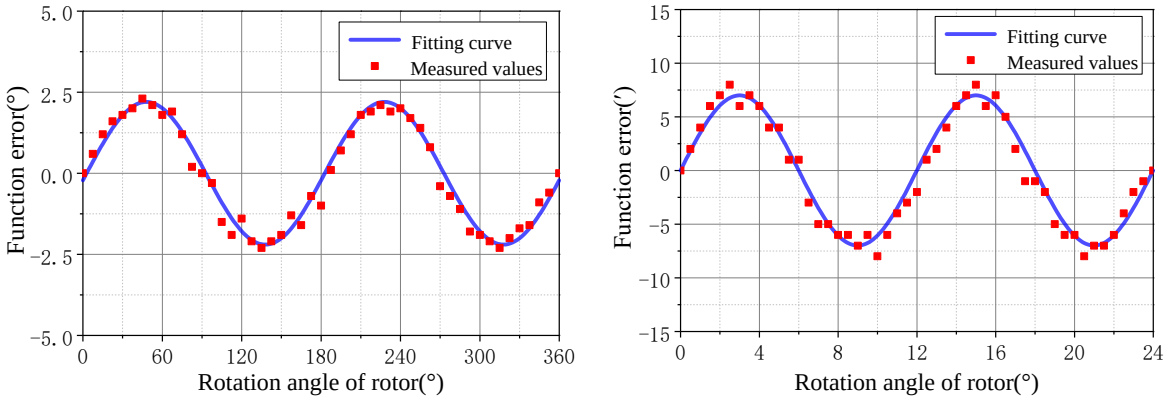


Figure 12. Test platform.

3.1. Test of Stator Radial Eccentricity

Under the condition that the rotor is concentric with the turntable, the stator of the 15 pole pairs of the CARR is artificially made to have radial eccentricity. Taking the peak position of the function of precise machine sine signal windings as the radial eccentricity direction, the relative eccentricity is selected as 50%. The function error of 15 pole pairs of the CARR with stator radial eccentricity is tested.

The measurement results show that when the stator radial eccentricity occurs, the zero error of the output electromotive force of coarse machine signal windings is $\pm 1^{\circ}14'$, and the zero error of the output electromotive force of precise machine signal windings is $\pm 4'$. It can be seen from Figure 13 that when the stator radial eccentricity occurs, the functional error of the output electromotive force of precise machine sine signal windings is $\pm 8'$, and the functional error of the output electromotive force of coarse machine sine signal windings is $\pm 2^{\circ}18'$. The measured results are consistent with the simulation results. The radial eccentricity of the stator will not only cause additional function errors, but also cause additional zero position errors.

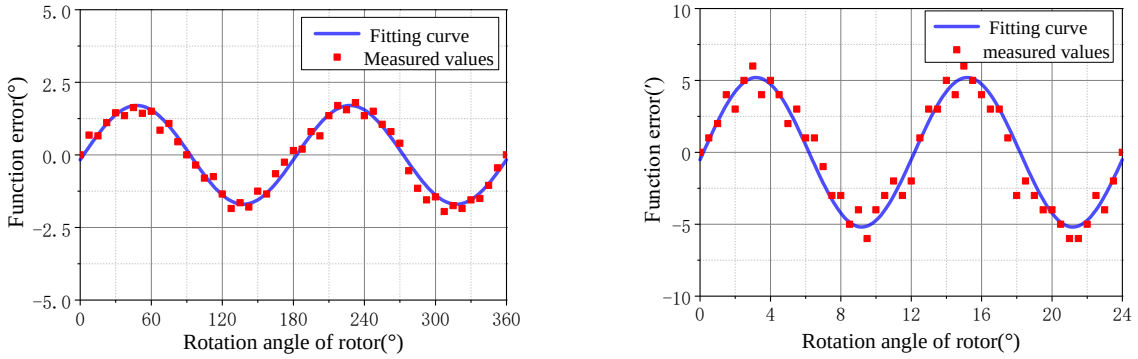


(**a**) Sine signal winding of coarse machine (**b**) Sine signal winding of precise machine

Figure 13. Measurement results of function error when radial eccentricity of stator exists.

3.2. Test of Rotor Radial Eccentricity

The radial eccentricity test of the rotor needs to ensure that the rotor of the 15 pole pairs of the CARR is eccentric artificially when the stator and the turntable are concentric. In order to facilitate measurement, the center line of the maximum wave crest of the rotor is taken as the eccentric direction, and the eccentricity is set as 50%. The functional error of 15 pole pairs of the CARR with radial eccentricity of the rotor is measured, and the measurement results are shown in Figure 14.



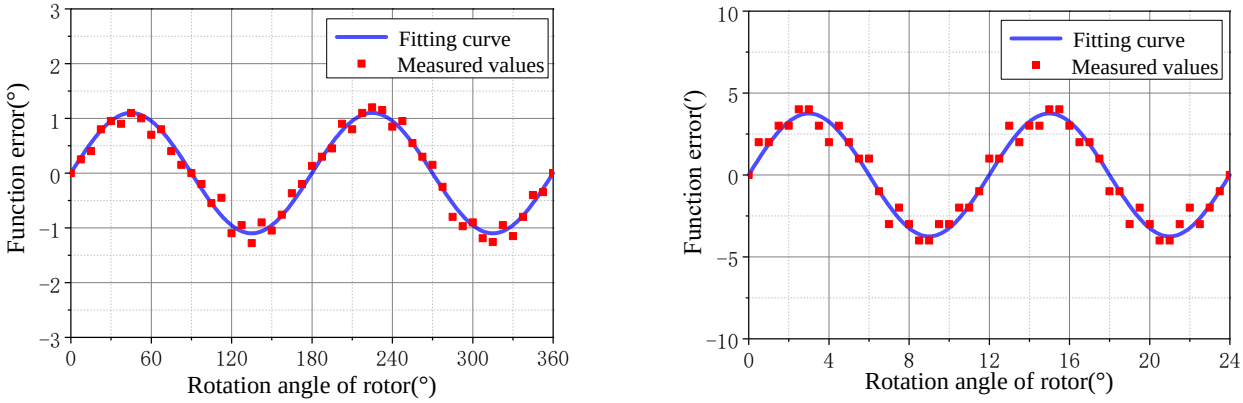
(**a**) Sine signal winding of coarse machine (**b**) Sine signal winding of precise machine

Figure 14. Measurement results of function error when radial eccentricity of rotor exists.

As can be seen from Figure 14, in the case of the radial eccentricity of the rotor, the function error of the output electromotive force of coarse machine sine signal windings is ±1°52′, and that of the output electromotive force of precise machine sine signal windings is ±6′. When the rotor is eccentrically radial, the zero error of the output electromotive force of coarse machine signal windings is about ±37′, and the zero error of the output electromotive force of precise machine signal windings is about ±2′. Compared with the case without eccentricity, the zero error of the CARR does not change when the rotor is eccentrically radial. However, the function error becomes larger at the same time, so the measurement accuracy of the CARR decreases.

3.3. Test of Rotor Axial Offset

The rotor axial offset of the 15 pole pairs of the CARR is set to 2mm, and its zero position error and function error are measured. The measurement results are shown in Figure 15.



(**a**) Sine signal winding of coarse machine (**b**) Sine signal winding of precise machine

Figure 15. Measurement results of function error when axial offset of rotor exists.

It can be seen from the measurement results that when the axial offset of the rotor is within 50% of the stator teeth height, the zero position error and function error of the 15 pole pairs of the CARR are basically the same as those without the offset. Therefore, when it is ensured that the rotor axial offset is within 50% of the stator teeth height, it can be considered that the rotor axial offset will not affect the measurement accuracy of the CARR.

4. Conclusions

In this paper, the influence of stator radial eccentricity, rotor radial eccentricity and rotor axial offset on the measurement accuracy of the CARR was studied, and an analysis method of finite element simulation was proposed to compare the stability of the signal output performance under two different winding modes, so as to provide reference for the design optimization of the CARR and other kinds of resolvers. The results show that the signal windings with the sine winding mode have a higher anti-eccentric interference performance than those with a winding mode of equal turns, and have a lower THD while maintaining a higher EMF amplitude. The errors caused by the stator radial eccentricity and rotor radial eccentricity exhibit directional variation patterns. The CARR has good robustness to rotor axial offset. Finally, the effectiveness of this finite element simulation analysis method for stator radial eccentricity, rotor radial eccentricity, and rotor axial offset was verified through experimental verification.

Author Contributions: H.W. proposed the research topic, designed the model, performed the simulations and analyzed the data. J.W. was responsible for guidance, proposing the research topic, giving constructive suggestions, and revising the paper. Z.Z. performed the simulations and analyzed the data. C.L. polished the manuscript and corrected spelling and grammar mistakes. All authors have read and agreed to the published version of the manuscript.

Funding: This work is supported by the Shandong Provincial Natural Science Foundation, ZR2020QE219.

Data Availability Statement: Data are contained within the article.

Conflicts of Interest: The authors declare no conflicts of interest.

References

1. Wang, S.; Kang, J.; Degano, M.; Buticchi, G. A resolver-to-digital conversion method based on third-order rational fraction polynomial approximation for PMSM control. *IEEE Trans. Ind. Electron.* **2019**, *66*, 6383–6392. [CrossRef]
2. Li, Z.; Xu, Y.; Fang, S.; Zheng, X.; Feng, X. Robust Operation of a Hybrid AC/DC Multi-energy Ship Microgrid with Flexible Voyage and Thermal Loads. *IEEE Trans. Smart Grid* **2020**, *11*, 2782–2793. [CrossRef]
3. Alipour-Sarabi, R.; Nasiri-Gheidari, Z.; Oraee, H. Development of a three-dimensional magnetic equivalent circuit model for axial flux machines. *IEEE Trans. Ind. Electron.* **2020**, *67*, 5758–5767. [CrossRef]
4. Saneie, H.; Nasiri-Gheidari, Z.; Belahcen, A. On the field reconstruction method for electromagnetic modeling of resolvers. *IEEE Trans. Instrum. Meas.* **2023**, *72*, 1–8. [CrossRef]
5. Li, Z.; Xu, Y.; Fang, S.; Mazzoni, S. Optimal Placement of Heterogeneous Distributed Generators in a Grid-Connected Multi-Energy Microgrid under Uncertainties. *IET Renew. Power Gener.* **2019**, *13*, 2623–2633. [CrossRef]
6. Zare, F.; Nasiri-Gheidari, Z. Helical motion wound-rotor resolver. *IEEE Sens. J.* **2022**, *22*, 9371–9377. [CrossRef]
7. Bahari, M.; Nasiri-Gheidari, Z.; Tootoonchian, F. Modeling, performance analyzing, and prototyping of variable reluctance resolver with toroidal winding. *IEEE Sens. J.* **2021**, *21*, 4425–4432. [CrossRef]
8. Sun, L.; Taylor, J.; Guo, X.; Cheng, M.; Emadi, A. Alinear positionmeasurement scheme for long-distance and high-speed applications. *IEEE Trans. Ind. Electron.* **2021**, *68*, 4435–4447. [CrossRef]
9. Xiao, L.F.; BI, C. An Optimization Approach of Rotor Contour for Variable Reluctance Resolver. *CES Trans. Electr. Mach. Syst.* **2021**, *5*, 257–261. [CrossRef]
10. Fateme, Z.; Ali, K.; Zahra, N.-G. Presentation of a Novel Variable Reluctance Tubular Resolver. *IEEE Trans. Ind. Electron.* **2022**, *69*, 13773–13780.
11. Reza, F.; Farid, T. Design and Experimental Investigation of a Two-DOF Planar Resolver. *IEEE Trans. Instrum. Meas.* **2022**, *71*, 9000408.
12. Ghaem-Maghami, M.; Nasiri-Gheidari, Z. Design Optimization of Linear Variable-Reluctance Resolver for Higher Accuracy and Smaller Size. *IEEE Sens. J.* **2023**, *23*, 16764–16771. [CrossRef]
13. Xiao, L.; Li, Z.; Bi, C. An Optimization Approach to Variable Reluctance Resolver. *IEEE Trans. Magn.* **2020**, *56*, 7509005.
14. Ran, X.; Zhao, M.; Shang, J. A novel axial reluctance resolver proposal and its winding configuration optimization using winding function method. *Energy Rep.* **2022**, *8*, 705–712. [CrossRef]
15. Cai, Y.; Ni, R.; Zhu, W.; Liu, Y. Modified Approach to Inductance Calculation of Variable Reluctance Resolver Based on Segmented Winding Function Method. *IEEE Trans. Ind. Appl.* **2023**, *59*, 5900–5907. [CrossRef]
16. Shi, Y.; Yu, Y.; Li, H.; Chen, Y. Position Self-Correction of Resolver Based on a Composite Method in Gimbal System. *IEEE Sens. J.* **2023**, *23*, 5412–5421. [CrossRef]
17. Hamed, L.; Zahra, N.-G.; Farid, T. Online Static/Dynamic Eccentricity Fault Diagnosis in Inverter-Driven Electrical Machines Using Resolver Signals. *IEEE Trans. Energy Convers.* **2020**, *35*, 1973–1980.
18. Khajueezadeh, M.S.; Emadaleslami, M.; Tootoonchian, F. Comprehensive Investigation of the Resolver's Eccentricity Effect on the Field-Oriented Control of PMSM. *IEEE Sens. J.* **2023**, *23*, 19145–19152. [CrossRef]
19. Emadaleslami, M.; KhajueeZadeh, M.; Tootoonchian, F. Static Eccentricity Fault Location Diagnosis in Resolvers Using Siamese-Based Few-Shot Learning. *IEEE Trans. Instrum. Meas.* **2023**, *72*, 9004209. [CrossRef]
20. Bahari, M.; Davoodi, A.; Saneie, H.; Tootoonchian, F.; Nasiri-Gheidari, Z. A new variable reluctance PM-Resolver. *IEEE Sens. J.* **2020**, *20*, 135–142. [CrossRef]
21. Khajuee Zadeh, M.; Saneie, H.; Nasiri-Gheidari, Z. Development of a hybrid reference model for performance evaluation of resolvers. *IEEE Trans. Instrum. Meas.* **2021**, *70*, 9004008.
22. Wang, K.; Wu, Z. Oversampling synchronous envelope detection for Resolver-to-Digital conversion. *IEEE Trans. Ind. Electron.* **2020**, *67*, 4867–4876. [CrossRef]
23. Moheyseni, A.; Nasiri-Gheidari, Z.; Alipour-Sarabi, R. Slotless disk type resolver: Asolution to improve the accuracy of multi-speedwound rotor resolvers. *IEEE Trans. Transp. Electrific.* **2022**, *8*, 1493–1500. [CrossRef]
24. Saneie, H.; Nasiri-Gheidari, Z.; Tootoonchian, F.; Daniar, A. Simplified winding arrangement for integrated multiturn resolvers. *IEEE Trans. Ind. Electron.* **2021**, *68*, 12802–12809. [CrossRef]

25. Sun, L.; Luo, Z.; Hang, J.; Ding, S.; Wang, W. A slotless PM variable reluctance resolver with axial magnetic field. *IEEE Trans. Ind. Electron.* **2020**, *69*, 6329–6340. [CrossRef]
26. Naderi, P.; Ghandehari, R.; Heidary, M. A comprehensive analysis on the healthy and faulty two types VR-resolvers with eccentricity and interturn faults. *IEEE Trans. Energy Convers.* **2021**, *36*, 3502–3511. [CrossRef]

Disclaimer/Publisher's Note: The statements, opinions and data contained in all publications are solely those of the individual author(s) and contributor(s) and not of MDPI and/or the editor(s). MDPI and/or the editor(s) disclaim responsibility for any injury to people or property resulting from any ideas, methods, instructions or products referred to in the content.